Charmed Meson Production in Deep Inelastic Scattering

B. Flöter,[1] B. Z. Kopeliovich,[2,3] H.-J. Pirner,[1,4] and J. Raufeisen[1]

[1] *Institute for Theoretical Physics, University of Heidelberg, Philosophenweg 19, 69120 Heidelberg, Germany*

[2] *Departamento de Física y Centro de Estudios Subatómicos, Universidad Técnica Federico Santa María, Casilla 110-V, Valparaíso, Chile*

[3] *Joint Institute for Nuclear Research, Dubna, Russia*

[4] *Max-Planck-Institut für Kernphysik, Saupfercheckweg 1, 69117 Heidelberg, Germany*

(Dated: February 1, 2008)

Abstract

Charmed meson production in semi-inclusive deep inelastic scattering is investigated in the color dipole formalism. The transverse momentum distributions are calculated. We find good agreement with the H1 data using a hard fragmentation function.

I. INTRODUCTION

One of the most important heavy-flavor production processes is deep inelastic scattering (DIS). A quantitative understanding of heavy-flavor physics in ep and pp-collisions is a prerequisite for the discovery of new effects in pA and AA-collisions. The color dipole model represents a good phenomenological approach to heavy-flavor production. In this model, the DIS cross section is factorized into a light-cone wavefunction, which describes the splitting of the virtual photon into a colorless quark-antiquark dipole with transverse separation r and a dipole cross section which depends on r and describes subsequent dipole scattering off the proton. The dipoles are eigenstates of the interaction and thus, multiple scattering effects on nuclei are easily described [1]. Historically, this was the initial intention to develop the dipole formalism. The dipole approach can be formulated in the target rest frame. For low-x the typical propagation length of a dipole fluctuation exceeds the interaction time by orders of magnitude. Because of time dilatation we can think of a frozen transverse separation during the interaction with the target. It is expected that the growth of the gluon density is slowed down at very low x_B by gluon-gluon recombination. Within the dipole approach, this saturation effect is described most naturally by introducing an x-dependent saturation scale. A fast-moving dipole produced from the incident virtual photon decouples from soft QCD interactions. This color transparency manifests itself in the dependence of the dipole cross section proportional to r^2 for small dipoles. The color dipole approach is inherently nonperturbative and includes higher twist effects which are important at low x-Bjorken and for low transverse momenta of the produced D-mesons.

The paper is organized as follows. Section 2 deals with D-meson production in deep inelastic scattering. We develop the kinematic framework for the description of semi-inclusive deep inelastic scattering. Section 3 introduces the dipole approach to DIS and presents the virtual photon-proton cross section preparing the numerical evaluation of the deep inelastic cross sections. In section 4 we finalize the dipole calculation and compare with data from HERA's H1 collaboration. Finally, in section 5 we summarize the results.

II. SEMI-INCLUSIVE D-MESON PRODUCTION IN DEEP INELASTIC SCATTERING

In inclusive Deep Inelastic Scattering (DIS) we consider the process $l\,N \to l'\,X$, where a lepton l with momentum k scatters off the nucleon N with momentum P resulting in a momentum k' for the scattered lepton l'. The target breaks up into an unobserved final state X. The cross section is most conveniently expressed in terms of the Lorentz invariants

$$Q^2 = -q^2 = -(k-k')^2 > 0 \qquad \nu = \frac{P\cdot q}{M} \tag{1}$$

or the ratios

$$x_B = \frac{Q^2}{2M\nu} \qquad y = \frac{P\cdot q}{P\cdot k}. \tag{2}$$

In the target rest frame, i.e. in the rest frame of the nucleon, ν gives the energy transfer from the lepton to the nucleon and y the ratio of energy transfer to incident lepton energy. Q^2 is the virtual mass squared (virtuality) of the exchanged photon. We also use the center-of-mass energy squared in the $l\,N$ system s and in the $\gamma^* p$ system

$$s = (k+P)^2, \qquad W^2 = (q+P)^2. \tag{3}$$

In Semi-inclusive Deep Inelastic Scattering (SIDIS) [2, 3] of the type $lH \to l'hX$ the hadron h is detected in coincidence with the scattered electron e' in the final state. The corresponding situation is pictured in Fig. 1. The hadronic target H has mass M and four-momentum P, the produced hadron h has mass m and four-momentum p_h.

The SIDIS cross section can be expressed in the same Lorentz invariants x_B and y as for inclusive DIS plus the final state hadron variables p_h. Since we aim for p_T factorization we split the final state hadron variables into the Lorentz invariant z momentum fraction of the hadron relative to the struck quark

$$z = \frac{P\cdot p_h}{P\cdot q} \tag{4}$$

and the transverse hadron momenta $p_{h_\perp}$ relative to the γ^* momentum direction. Both are invariant under boosts along the virtual photon axis. The differentials are related by

$$\frac{d^3p_h}{2E_h} = \frac{1}{4}\frac{\nu}{p_{h||}} dz dp_{h\perp}^2 d\phi_h. \tag{5}$$

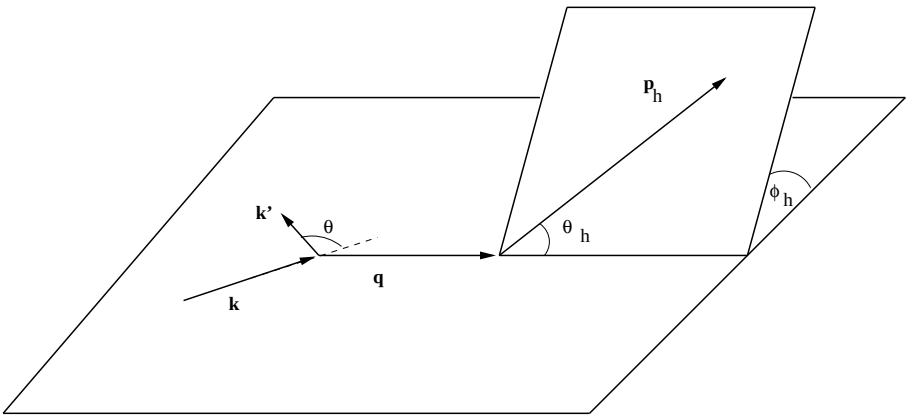

FIG. 1: Kinematics of one-particle semi-inclusive scattering. The reaction plane in $(e, e'h)$-scattering is defined by the initial and final momenta of the lepton $(\vec{k}, \vec{k}')$. The produced hadron $\vec{p}_h$ and photon momenta $\vec{q}$ define a second plane.

In analogy to inclusive DIS the SIDIS cross section can be obtained from the contraction of the hadronic and the leptonic tensor

$$\begin{aligned} \frac{2E_h\, d\sigma}{d^3p_h\, dx_B\, dy} &= \frac{\pi\alpha^2 2My}{Q^4} L_{\mu\nu} W^{\mu\nu} \\ \frac{2E_h\, d\sigma}{d^3p_h\, d\Omega\, dE'} &= \frac{\alpha^2}{Q^4} L_{\mu\nu} W^{\mu\nu}. \end{aligned} \tag{6}$$

The conversion between these two forms is given by the Jacobian

$$dx_B dy = \frac{E'}{M(E-E')} dE' d\cos\theta$$

for azimuthal symmetry. $L_{\mu\nu}$ is the spin averaged leptonic tensor and $W_{\mu\nu}$ is the hadronic tensor

$$\begin{aligned} W_{\mu\nu} &= \frac{1}{2M(2\pi)^4} \int \frac{d^3P_X}{(2\pi)^3 2E_X} < P|J_\nu(0)|P_X, p_h >< p_h, P_X|J_\mu(0)|P > \\ &\times\ (2\pi)^4 \delta^4(P + q - p_h - P_X). \end{aligned} \tag{7}$$

The semi-inclusive hadronic tensor is related to the inclusive one via

$$< n_h(P,q) > \underline{W_{\mu\nu}}(P,q) = \int \frac{d^3p_h}{2E_h} W_{\mu\nu}(P,q,p_h) \tag{8}$$

where $< n_h(P,q) >$ is the average number of particles produced of type h in a reaction defined by P and q. The above notation underlines the dependence on the momenta of

the deep inelastic reaction. Integrating over the hadron momentum p_h one recovers the inclusive hadronic tensor times the multiplicity as shown on the right hand side of Eq. 8. Summation over all possible hadrons h would lead to the inclusive hadronic tensor. The tensorial structure of $W_{\mu,\nu}$ is determined by Lorentz and gauge invariance.

Assuming time reversal and parity invariance we represent the electromagnetic hadronic tensor with four structure functions $W_i(x, Q^2, z, \vec{p}_h^{\,2})$ [2]

$$\begin{aligned} W_{\mu\nu}(P, p_h, q) &= (\frac{q_\mu q_\nu}{q^2} - g_{\mu\nu})W_1 + \frac{T_\mu T_\nu}{M^2}W_2 \\ &+ \frac{p^\perp_{h\mu}T_\nu + T_\mu p^\perp_{h\nu}}{M m_h}W_3 + \frac{p^\perp_{h\mu}p^\perp_{h\nu}}{m_h^2}W_4 \end{aligned} \tag{9}$$

where

$$T^\mu = P^\mu - \frac{p\cdot q}{q^2}q^\mu. \tag{10}$$

The first two structure functions have the same origin as in the inclusive structure functions which are related to longitudinal and transverse photon scattering. The dependence on the hadronic angle ϕ_h allows two more structure functions. Next we introduce four dimensionless semi-inclusive structure functions $H_i(x, Q^2, z, p^2_{h\perp})$. A factor of $2z$ arises in formal analogy to the known inclusive structure functions $F_{1,2}$

$$\begin{aligned} 2zH_1 &= M(W_1 + \frac{p^2_{h\perp}}{2m_h^2}W_4) \\ 2zH_2 &= \nu(W_2 + \frac{p^2_{h\perp}Q^2}{2m_h^2\vec{q}^2}W_4). \end{aligned} \tag{11}$$

The integration over the azimuthal angle ϕ_h removes the H_3 and H_4 structure functions from the semi-inclusive cross section

$$\begin{aligned} H_i(x_B, Q^2, z) &= \frac{1}{2}\int dp^2_{h\perp}d\phi_h H_i(x_B, Q^2, z, p^2_{h\perp}) \\ &= \pi\int dp^2_{h\perp}H_i(x_B, Q^2, z, p^2_{h\perp}) \end{aligned} \tag{12}$$

which leads to

$$\frac{d\sigma}{dx_B\,dz\,dy} = \frac{8\pi\alpha^2 ME}{Q^4}\left[\, x_B y^2 H_1(x_B, Q^2, z, p^2_{h\perp}) + (1-y)H_2(x_B, Q^2, z, p^2_{h\perp})\,\right]. \tag{13}$$

In the high-energy approximation $E = s/(2M)$ the cross section has a form similar to the inclusive cross section. Factorization of deep inelastic scattering and hadronization allows to

represent the inclusive structure function H_2 as a product of the known quark distribution functions and the quark fragmentation function $D_{h/q_f}(z)$ [4]

$$H_2(x_B, Q^2, z) = H_2(x_B, z) = \sum_f e_f^2 [q_{f/H}(x_B) D_{h/q_f}(z) + \bar{q}_{f/H}(x_B) D_{h/\bar{q}_f}(z)]. \tag{14}$$

This factorization has been proven to leading order in Q [3]. Here, in this paper, we want to calculate the structure functions H_i in the dipole formalism for $\gamma^* p$. Using equation (8), we connect the H_i to the standard structure functions F_i for inclusive lepton-hadron scattering,

$$\begin{aligned} < n_h(x_B, Q^2) > F_1(x_B, Q^2) &= \int dz\, H_1(x_B, z, Q^2) \\ < n_h(x_B, Q^2) > F_2(x_B, Q^2) &= \int dz\, H_2(x_B, z, Q^2). \end{aligned} \tag{15}$$

Following the inclusive case, we need two structure functions specified for longitudinal and transverse photon polarization. Polarization interference in semi-inclusive DIS occurs only for W_3 and W_4 which vanish after integration over the azimuthal angle.

$$\begin{aligned} W_L &= \varepsilon(\lambda = 0) \cdot W \cdot \varepsilon(\lambda = 0) = 2z \left(\frac{\vec{q}^2}{\nu Q^2} H_2 - \frac{1}{M} \right) \\ W_T &= \frac{1}{2} \left[\varepsilon(\lambda = -1) \cdot W \cdot \varepsilon(\lambda = -1) + \varepsilon(\lambda = +1) \cdot W \cdot \varepsilon(\lambda = +1) \right] = \frac{2z}{M} H_1 \end{aligned} \tag{16}$$

where ε is the virtual photon polarization vector. For the virtual photon momentum $q = (q^0, 0, 0, q^z)$ we define the polarization vectors:

$$\varepsilon(\lambda = 0) = \frac{1}{Q} \left(q^z, 0, 0, q^0 \right) \qquad \varepsilon(\lambda = \pm 1) = \frac{1}{\sqrt{2}} (0, 1, \pm i, 0). \tag{17}$$

The combined longitudinal and transverse electron-proton cross section is

$$\frac{d\sigma}{dx_B\, dz\, dy\, dp_{h\perp}^2\, d\phi_h} = \frac{\pi \alpha^2 M}{2Q^2 yz} \left\{ \left(\frac{y^2}{2} + 1 - y \right) W_T + (1 - y) W_L \right\}. \tag{18}$$

We recall the relation between the total $\gamma^* p$ cross section and the inclusive hadronic tensor $W^{\mu\nu}(P, q)$

$$\sigma^{tot}_{\gamma^* p \to X}(\lambda) = \frac{16 \pi^2 \alpha M}{2ys} \varepsilon^*_\mu(\lambda) W^{\mu\nu}(P, q) \varepsilon_\nu(\lambda). \tag{19}$$

Since the amount of D-meson production is measured by the branching ratio

$$< n_D >= \frac{1}{\sigma^{tot}_{\gamma^* p \to X}(\lambda)} \int dy\, \frac{\partial \sigma^{inc}_{\gamma^* p \to D\, X}(\lambda)}{\partial y} \tag{20}$$

we obtain

$$\frac{2E_D\, d\sigma^{\gamma^* p \to DX}}{d^3 p_D} = \frac{8\pi^2 \alpha M}{ys} \varepsilon^*_\mu(\lambda) W^{\mu\nu}(P, q, p_D) \varepsilon_\nu(\lambda), \tag{21}$$

or with (5)

$$\frac{ysz}{\pi^2 M\alpha_{em}}\frac{d\sigma^{L,T}}{d^2p_D\,dz} = \varepsilon^{L,T}\cdot W\cdot\varepsilon^{L,T}. \tag{22}$$

We insert this expression in (18) to find

$$\begin{aligned}\frac{d\sigma(ep\to DX)}{dx\,dy\,dz\,d^2p_D^\perp} &= \frac{\alpha_{em}}{\pi xy}\left[\left(\frac{y^2}{2}-y+1\right)\frac{d\sigma^T(\gamma^*p\to DX)}{dz\,d^2p_D^\perp}\right.\\ &\quad\left.+\;(1-y)\,\frac{d\sigma^L(\gamma^*p\to DX)}{dz\,d^2p_D^\perp}\right].\end{aligned} \tag{23}$$

This equation relates the SIDIS cross section to the semi-inclusive cross section of a virtual photon on the proton. The latter can easily be calculated in the color dipole model, since the photon is the source of the color dipole, and the target proton mainly delivers the low x-gluon which is necessary for the virtual heavy quark-antiquark state in the photon to materialize.

III. D-MESON PRODUCTION IN THE COLOR-DIPOLE MODEL

The γ^*p charm quark production cross section is calculated in the dipole model (cf. ref. [22]). We start with the photon-gluon-fusion processes shown in fig. 2. The respective Feynman graphs are represented by the amplitudes M_1^μ and M_2^μ

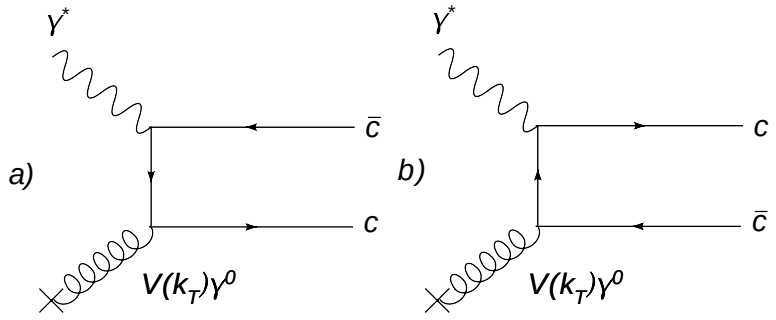

FIG. 2: Boson-Gluon-Fusion graphs. FIG (2a) shows iM_1, FIG (2b) iM_2.

$$\begin{aligned}iM_1^\mu &= -\sum_\sigma \varepsilon_\mu(\lambda)\bar u_{\sigma_q}(p_q)V(k_t)\gamma^0\frac{u_\sigma(q-p_{p_{\bar q}})\bar u_\sigma(q-p_{p_{\bar q}})}{(q-p_{\bar q})^2-m^2}ee_Q\gamma^\mu v_{\sigma_{\bar q}}(p_{\bar q})\\ iM_2^\mu &= \sum_\sigma \varepsilon_\mu(\lambda)\bar u_{\sigma_q}(p_q)ee_Q\gamma^\mu\frac{v_\sigma(q-p_q)\bar v_\sigma(q-p_q)}{(q-p_{\bar q})^2-m^2}V(k_t)\gamma^0 v_{\sigma_{\bar q}}(p_{\bar q}).\end{aligned} \tag{24}$$

Here $\varepsilon(\lambda)$ is the polarization vector of the virtual photon γ^* with polarization λ, $u_{\sigma_q}(p_q)$ the spinor of the heavy quark with helicity σ_q and momentum p_q, and $v_{\sigma_{\bar{q}}}(p_{\bar{q}})$ the spinor of the antiquark with helicity $\sigma_{\bar{q}}$ and momentum $p_{\bar{q}}$. The charge of the heavy quark in units of e is e_Q. The polarization vectors are given in eqs. (17). The target color field represented by the vertex function $V(k_t)$ depends on the transverse momentum k_t injected by the gluon from the target. The vertex V is restricted to its time-component, i.e. the formula holds only in the target rest frame. It is assumed that the target gluon mediates transverse momentum only, longitudinal momentum and energy transfers are negligible. In the high-energy approximation the fermion propagators can be treated onshell [5]. This approximation is equivalent to neglecting the instantaneous terms in light-cone quantization [6]. We can express the energy denominators in terms of LC variables. The coordinate system is chosen such that the z-axis points in $\vec{q}$-direction. With the light-cone momentum of the photon $(q^+, 0_\perp, q^-) = (Q^2/(2mx_B), 0, -mx_B)$ and α as the light-cone momentum fraction of the quark we find $(p_q^+, p_{q\perp}, p_q^-) = (\alpha q^+, p_{q\perp}, (p_{q\perp}^2 + m^2)/(\alpha q^+))$. This allows to simplify the propagators in eq. (24). Equivalent expressions hold for the antiquark with α replaced by $1-\alpha$

$$\begin{aligned}
\frac{1}{(q-p_q)^2 - m^2} &= \frac{-\alpha}{p_{q\perp}^2 + \epsilon^2} \\
\frac{1}{(q-p_{\bar{q}})^2 - m^2} &= \frac{\alpha - 1}{(p_{q\perp} - k_t)^2 + \epsilon^2} \\
\epsilon^2 &= \alpha(1-\alpha)Q^2 + m^2. \qquad (25)
\end{aligned}$$

The parameter ϵ^2 is related to the inverse extension squared of the quark-antiquark state.

The $\gamma^* p$ cross section is proportional to the absolute square of the summed transition amplitudes M_i^μ. In the phase space integration we use the integration variable k_t given by the equation $k_t = p_q + p_{\bar{q}} - q$ instead of $p_{\bar{q}}$:

$$d^5\sigma = \sum_{\sigma_q \sigma_{\bar{q}} c_q c_{\bar{q}} \lambda, \lambda'} \frac{d\alpha\, d^2p_q^\perp\, d^2k_t}{8(2\pi)^5 (q^0)^2 \alpha(1-\alpha)} \epsilon_\mu^*(\lambda)\epsilon_\nu(\lambda')(M_1^\mu + M_2^\mu)(M_1^{*\nu} + M_2^{*\nu}.) \qquad (26)$$

The polarization-interference terms vanish when integrated over the azimuthal angle. It is advantageous to transform all expressions into impact parameter space since at high energies the quarks propagate along fixed impact parameter trajectories. We express the vector amplitudes $M_i^\mu(\vec{k}_t, \vec{p}_q)$ by their Fourier transforms $\tilde{M}_i^\mu(\vec{b}, \vec{r})$ in eq. (27)

$$M_i^\mu(\vec{k}_t,\vec{p}_q) = \int d^2b d^2r \tilde{M}_i^\mu(\vec{b},\vec{r}) \mathrm{e}^{i\vec{k}_t\vec{b}+i\vec{p}_q^\perp\vec{r}}. \tag{27}$$

The explicit form of the vector amplitudes in coordinate space is:

$$\begin{aligned}
\tilde{M}_1^\mu(\vec{b},\vec{r}) &= -i2p_q^0 ee_Q(1-\alpha)\int \frac{d^2k_t\, d^2p_q^\perp}{(2\pi)^4}\,\mathrm{e}^{-i\vec{k}_t\vec{b}-i\vec{p}_q^\perp\vec{r}}\,V(k_t) \\
&\times \quad \frac{\bar{u}_{\sigma_q}(q-p_{\bar{q}})\gamma^\mu v_{\sigma_{\bar{q}}}(p_{\bar{q}})}{(p_{q\perp}-k_t)^2+\epsilon^2} \\
\tilde{M}_2^\mu(\vec{b},\vec{r}) &= i2p_{\bar{q}}^0 ee_Q\alpha\int \frac{d^2k_t\, d^2p_q^\perp}{(2\pi)^4}\,\mathrm{e}^{-i\vec{k}_t\vec{b}-i\vec{p}_q^\perp\vec{r}}\,V(k_t) \\
&\times \quad \frac{\bar{u}_{\sigma_q}(p_q)\gamma^\mu v_{\sigma_{\bar{q}}}(q-p_q)}{p_{q\perp}^2+\epsilon^2}.
\end{aligned} \tag{28}$$

With the vertex function in impact parameter space

$$\tilde{V}(\vec{b}) = \int \frac{d^2k_t}{(2\pi)^2}\exp(-i\vec{k}_t\vec{b})V(\vec{k}_t)$$

and the light-cone wave function:

$$\Psi^\mu(\vec{r}) = e_Q\sqrt{\alpha_{em}}\sqrt{N_c}\sqrt{\alpha(1-\alpha)}\int\frac{d^2p_q^\perp}{(2\pi)^2}\,\mathrm{e}^{-\vec{p}_q^\perp\vec{r}}\,\frac{\bar{u}_{\sigma_q}(p_q)\gamma^\mu v_{\sigma_{\bar{q}}}(q-p_q)}{p_{q\perp}^2+\epsilon^2} \tag{29}$$

one finds that the momentum space integrals factorize and yield the convenient expressions:

$$\begin{aligned}
\tilde{M}_1^\mu(\vec{b},\vec{r}) &= -i2p_q^0\sqrt{\tfrac{1-\alpha}{\alpha}}\sqrt{\tfrac{4\pi}{N_c}}\tilde{V}(\vec{b}+\vec{r})\Psi^\mu(\vec{r}) \\
\tilde{M}_2^\mu(\vec{b},\vec{r}) &= i2p_{\bar{q}}^0\sqrt{\tfrac{\alpha}{1-\alpha}}\sqrt{\tfrac{4\pi}{N_c}}\tilde{V}(\vec{b})\Psi^\mu(\vec{r}).
\end{aligned} \tag{30}$$

The light-cone wave function Ψ^μ describes the splitting $\gamma^* \to q\bar{q}$ and appears identically in both initial state amplitudes. The vertex function has the respective arguments b and $b+r$ which are the impact parameters of the antiquark in M_2 and M_1. Using $p_q^0 \approx \alpha q^0$, $p_{\bar{q}}^0 \approx (1-\alpha)q^0$, we find for the $\gamma^* p$ production cross section of a heavy quark with momentum p_q

$$\begin{aligned}
\frac{d\sigma^{L,T}}{d^2p_q^\perp} &= \int\frac{1}{(4\pi)^2}\int d^2b d^2r_1\, d^2r_2 d\alpha\,\mathrm{e}^{i\vec{p}_q^\perp(\vec{r}1-\vec{r}2)} \\
&\times\frac{1}{N_c}\sum_{c_q c_{\bar{q}}}\Psi^{L,T}(\vec{r}_1)\Psi^{*L,T}(\vec{r}_2)[\tilde{V}(\vec{b})-\tilde{V}(\vec{b}+\vec{r}_1)][\tilde{V}^\dagger(\vec{b}-\tilde{V}^\dagger(\vec{b}+\vec{r}_2)].
\end{aligned} \tag{31}$$

Due to the integration over the antiquark momentum which is equivalent to the k_t integration, the impact parameters in $(\tilde{M}_1^{\mu} + \tilde{M}_2^{\mu})$ and $(\tilde{M}_1^{*\nu} + \tilde{M}_2^{*\nu})$ coincide. Since the momentum of the quark p_q remains unintegrated, the exponentials of the Fourier transforms survive. The light-cone wave functions simplify after summation over spins and polarizations

$$\begin{aligned}
\Psi^L(\vec{r}_1)\Psi^{*L}(\vec{r}_2) &= \textstyle\sum_{\sigma_q\sigma_{\bar{q}}} \varepsilon_\mu(\lambda=0)\varepsilon^*_\nu(\lambda=0)\Psi^{\mu}(\vec{r}_1)\Psi^{*\nu}(\vec{r}_2) \\
\Psi^T(\vec{r}_1)\Psi^{*T}(\vec{r}_2) &= \tfrac{1}{2}\textstyle\sum_{\lambda=\pm\frac{1}{2}}\sum_{\sigma_q\sigma_{\bar{q}}} \varepsilon_\mu(\lambda)\varepsilon^*_\nu(\lambda)\Psi^{\mu}(\vec{r}_1)\Psi^{*\nu}(\vec{r}_2).
\end{aligned} \tag{32}$$

Combining the gluon vertex operators V appropriately we can construct dipole cross sections

$$\begin{aligned}
&\int d^2b[\tilde{V}(\vec{b}) - \tilde{V}(\vec{b}+\vec{r}_1)][\tilde{V}^\dagger(\vec{b}) - \tilde{V}^\dagger(\vec{b}+\vec{r}_2)] = \\
&\frac{1}{2}\int d^2b\left[\mid \tilde{V}(\vec{b}) - \tilde{V}(\vec{b}+\vec{r}_1)\mid^2 + \mid \tilde{V}(\vec{b}) - \tilde{V}(\vec{b}+\vec{r}_2)\mid^2 - \mid \tilde{V}(\vec{b}+\vec{r}_2) - \tilde{V}(\vec{b}+\vec{r}_1)\mid^2\right].
\end{aligned} \tag{33}$$

The corresponding absolute squares can be grouped into dipole cross sections employing the definition:

$$\sigma_{q\bar{q}}(r) = \frac{1}{N_c}\sum_{c_q c_{\bar{q}}}\int d^2b \mid \tilde{V}(\vec{b}) - \tilde{V}(\vec{b}+\vec{r})\mid^2 . \tag{34}$$

One finds the following final form for the differential γ^*p cross section for charm quark production, i.e. $q = c$:

$$\begin{aligned}
\frac{d\sigma^{L,T}(\gamma^* p \to (cX))}{d^2p_c^{\perp}} &= \frac{1}{(2\pi)^2}\int d^2r_1\, d^2r_2\, d\alpha\, \mathrm{e}^{i\vec{p}_c^{\,\perp}(\vec{r}_1-\vec{r}2)}\, \Psi^{L,T}(\vec{r}_1)\Psi^{*L,T}(\vec{r}_2) \\
&\times \frac{1}{2}\{\sigma_{c\bar{c}}(\vec{r}_1) + \sigma_{c\bar{c}}(\vec{r}_2) - \sigma_{c\bar{c}}(\vec{r}_1-\vec{r}_2)\}.
\end{aligned} \tag{35}$$

A similar expression has been derived in [7] to describe the transverse momenta of Drell-Yan pairs. In the differential cross section light-cone wave functions enter with Bessel functions K_0 and K_1 depending on $\varepsilon = \sqrt{m^2 + \alpha(1-\alpha)Q^2}$ and r_1 or r_2:

$$\begin{aligned}
\Psi^L(\alpha,r_1)\Psi^{*L}(\alpha,r_2) &= \frac{2N_c\alpha_{em}e_Q^2}{(2\pi)^2}\, 4Q^2\alpha^2(1-\alpha)^2 K_0(\epsilon r_1)K_0(\epsilon r_2) \\
\Psi^T(\alpha,r_1)\Psi^{*T}(\alpha,r_2) &= \frac{6e_Q^2\alpha_{em}}{(2\pi)^2}\{m_Q^2 K_0(\epsilon\vec{r}_1)K_0(\epsilon\vec{r}_2) \\
&+ \epsilon^2[\alpha^2 + (1-\alpha)^2]\frac{\vec{r}_1\vec{r}_2}{r_1 r_2}K_1(\epsilon\vec{r}_1)K_1(\epsilon\vec{r}_2)\}.
\end{aligned} \tag{36}$$

If one integrated out the transverse quark momentum in equation (35), one would find a delta function in $(r_1 - r_2)$ and recover the total cross section of charm production. The differential cross section does not have such an intuitive interpretation as the total DIS cross section. As shown in the derivation a physical quark-antiquark fluctuation is not a prerequisite for the appearance of the dipole cross section in the inclusive cross section. Instead, interference terms in the square of the transition amplitude produce dipole cross sections when a quark in the amplitude and a quark in the complex conjugate amplitude enter with different impact parameters. This becomes very obvious in the Drell-Yan process, where the dipole formula for the transverse momentum distribution of lepton pairs looks very similar to (35) although there is not necessarily any dipole fluctuation involved in the Feynman graphs [8].

We gave the inclusive DIS cross section in terms of the cross section of a quark-antiquark pair scattering off a proton. For the calculations in this paper we use a fit to the dipole cross section and its energy dependence. For an explicit derivation of the dipole cross section from QCD we refer to the loop-loop correlation model, see Ref. [9]. In the following we use the GBW-saturation model by Golec-Biernat and Wüsthoff [10] with a dipole-nucleon cross section of the form:

$$\sigma_{q\bar{q}}(x,r) = \sigma_0 \left[1 - \exp\left(-\frac{r^2}{4R_0^2(x)}\right)\right] \tag{37}$$

where

$$R_0 = \frac{1}{Q_0}\left(\frac{x}{x_0}\right)^{\frac{\lambda}{2}}. \tag{38}$$

This cross section is not a well-defined quantity for $Q^2 = 0$. Therefore, x has been modified

$$x \to x\left(1 + \frac{4m_Q^2}{Q^2}\right) \tag{39}$$

in order to describe the transition to the photoproduction region. The distance between the quark and antiquark is r. The inverse momentum $1/Q_0 = 0.2fm$ is a perturbative distance. At $x = x_0 = 0.41 * 10^{-4}$ twice this distance equals the distance where the cross section changes from the perturbative r^2 behavior into a constant behavior. The parameters λ, σ_0 and x_0 are given in Table (I) [10]. The fit is performed within a Bjorken interval $4 * 10^{-4} \leq x_B \leq 0.01$ and virtuality range of $0.1\text{GeV}^2 \leq Q^2 \leq 400\text{GeV}^2$.

The saturation model contains four fit parameters. This is a small number compared to the number of parameters in parton distribution functions. The authors have performed a

	σ_0 (mb)	λ	x_0	$1/Q_0(fm)$
$\sigma_{q\bar{q}}$ with charm	29.12	0.277	$0.41 \cdot 10^{-4}$	0.2

TABLE I: Fit parameters in the GBW saturation model [10]. The charm quark mass is fixed to $m = 1.5$GeV.

fit to HERA data and reached a satisfactory χ^2 in Ref. [10] containing charm in the sum over flavors.

The model describes two different saturation effects. The GBW cross section saturates for quark-antiquark pairs with large r separation. Arbitrarily large $q\bar{q}$-separations are not physical due to hadronization, but this does not matter, since they occur in the $q\bar{q}$ light-cone wave function with very low probability. The other saturation effect is implemented via the x-dependence of $R_0 \sim 1/Q_s$, where Q_s acts as a saturation scale. The $\gamma^* p$ cross section rises earlier to σ_0 for decreasing x. One expects this increase to be slowed down or stopped at even lower x when the gluon-gluon-recombination cross section becomes sizeable [11]. The color-glass model predicts a new QCD domain which is nonperturbative but not dominated by confinement effects. Note, both saturation effects are not to be mixed up with the saturation of the gluon density in impact parameter space discussed in Ref. [9].

For our calculations we can expand the cross section to first order in r^2

$$\sigma_{q\bar{q}}(x,r) \simeq \sigma_0 \frac{r^2}{4R_0^2(x)} =: \tilde{\sigma}_0 r^2, \tag{40}$$

where R_0 is given in (38). In the following we refer to this use of the color dipole cross section as r^2-approximation. For D-meson production with a charm mass $m = 1.5$ GeV, we do not expect that the size of the semi-inclusive cross section is very much influenced by large dipole separations. The dipoles contributing have a size of about 0.2 fm.

IV. NUMERICAL CALCULATION

With the analytical formulae and the above dipole cross section we can numerically calculate the double differential charmed quark production cross section $d\sigma^{T,L}/d^2p_c^{\perp}$. We reduce the fourfold Fourier integral over $\vec{r}_1$, $\vec{r}_2$ which occurs in the $\gamma^* p$ sub cross section (35) to a one-dimensional integral over the dipole separation r. We find integrals with modified Bessel functions of the second kind $K_{0,1}$ and Bessel functions of the first kind $J_{0,1}$

$$\frac{d\sigma(\gamma^* p \to c\,X)}{d^2 p_c^\perp} = \frac{6 e_Q^2 \alpha_{em}}{(2\pi)^2} \int d\alpha \times \left\{ \left[m_c^2 + 4Q^2\alpha^2(1-\alpha)^2 \right] \left[\frac{I_1}{p_c^{\perp 2} + \epsilon^2} - \frac{I_2}{4\epsilon} \right] + \left[\alpha^2 + (1-\alpha)^2 \right] \left[\frac{p_c^\perp \epsilon I_3}{p_c^{\perp 2} + \epsilon^2} - \frac{I_1}{2} + \frac{\epsilon I_2}{4} \right] \right\} \tag{41}$$

with

$$\begin{aligned} I_1 &= \int dr\, r\, J_0(p_c^\perp r)\, K_0(\epsilon r)\, \sigma_{q\bar{q}}(r) \\ I_2 &= \int dr\, r^2\, J_0(p_c^\perp r)\, K_1(\epsilon r)\, \sigma_{q\bar{q}}(r) \\ I_3 &= \int dr\, r\, J_1(p_c^\perp r)\, K_1(\epsilon r)\, \sigma_{q\bar{q}}(r)\ . \end{aligned} \tag{42}$$

The small r^2-approximation (40) of the GBW dipole cross section allows to perform the r-integrations I_1-I_3 analytically

$$\begin{aligned} I_1|_{r^2-approx.} &= \frac{\sigma_0}{4R_0^2} \frac{4\,(\epsilon^2 - p_c^{\perp 2})}{(p_c^{\perp 2} + \epsilon^2)^3} \\ I_2|_{r^2-approx.} &= \frac{\sigma_0}{4R_0^2} \frac{16\,\epsilon\,(\epsilon^2 - 2p_c^{\perp 2})}{(p_c^{\perp 2} + \epsilon^2)^4} \\ I_3|_{r^2-approx.} &= \frac{\sigma_0}{4R_0^2} \frac{8\,p_c^\perp\,\epsilon}{(p_c^{\perp 2} + \epsilon^2)^3}\ . \end{aligned} \tag{43}$$

The integrals require an extension parameter ϵ greater than zero to be finite. For heavy-quark production with $\epsilon \geq m$ this is no problem. We have checked how much the approximate r^2-calculation and the full GBW dipole cross section differ for the sum of transversely and longitudinally polarized photons. In Fig. 3 we show the $\gamma^* p \to c\,X$ cross section in r^2-approximation over the same cross section calculated with the full GBW parametrization. Deviations appear mainly at low transverse momenta of less than about 1 GeV^2. We find good agreement for higher Q^2, when the average dipole size is small. Above $p_c^{\perp 2} > 2$ GeV^2 we find a very small deviation of maximally 2%, which is sufficient for our calculations.

Next, we study the relative contributions of longitudinally and transversely polarized virtual photons in Fig. 4. The transverse cross section is clearly dominating. The relative contribution of the longitudinal cross section grows when the virtuality of the photon changes from $Q^2 = 2$ GeV^2 to 100 GeV^2. This behavior is similar to vector meson production.

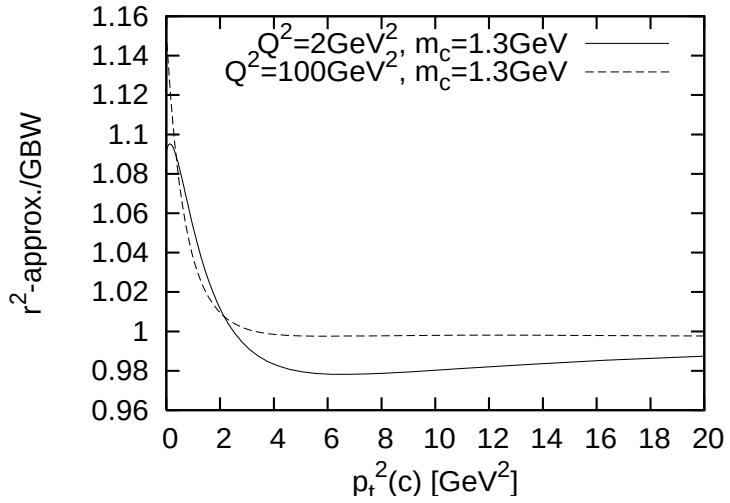

FIG. 3: The ratio of the cross section $d\sigma(\gamma^* p \to c\,X)/dp_c^{\perp 2}$ in r^2-approximation over the same cross section calculated with the full GBW cross section $\sigma(r)$ is shown as a function of the transverse momentum of the charm quark $p_c^{\perp 2}$.

To calculate D-meson cross sections we must let the charm quark fragment. The fragmentation function $D_h^Q(z^*)$ gives the probability that the original charm quark with a momentum P fragments into a D-meson with momentum fraction z^*P. All our momentum fractions in section 3 refer to the photon momentum q. Since we start with a charm quark of momentum $P = \alpha q$ and end up with a D-meson with momentum zq the momentum fractions multiply:

$$z = z^* \alpha. \tag{44}$$

To calculate D-meson production we convolute the charm quark production cross section $d\sigma^{L,T}(\gamma^* p \to cX)$ with the nonperturbative fragmentation function $D(z^*)$: $d\sigma^{L,T}(\gamma^* p \to DX)$

$$\frac{d\sigma^{L,T}}{dz\, d^2p_D^\perp}(\gamma^* p \to DX) \;=\; \int \frac{dp_c^\perp\, d\alpha}{\alpha}\, \frac{d\sigma^{L,T}}{d^2p_c^\perp\, d\alpha}(\gamma^* p \to cX) \tag{45}$$

$$\times\; D_D^c\left(\frac{z}{\alpha}\right)\, \delta\left(p_D^\perp - \frac{z}{\alpha}\, p_c^\perp\right)\;. \tag{46}$$

We use the Peterson fragmentation function [12] which has the form

$$D_Q^h(z^*) = \frac{n(h)}{z^*[1 - \frac{1}{z^*} - \frac{\epsilon_Q}{1-z^*}]^2}\;. \tag{47}$$

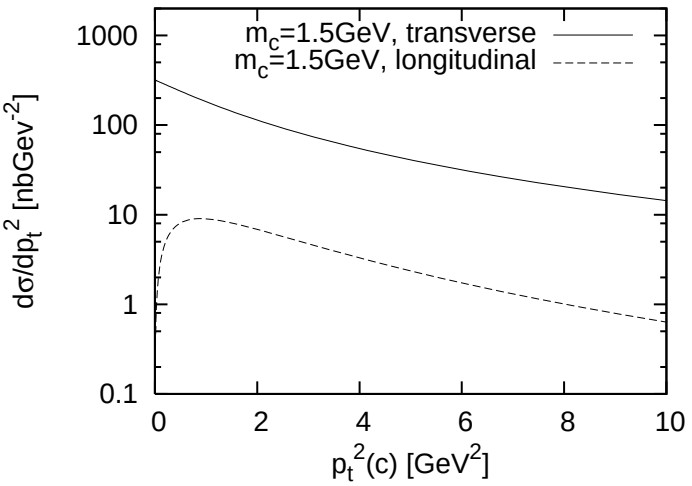

FIG. 4: The charm quark production cross section $\gamma^* p \to cX$ induced by transverse and longitudinal photons for $Q^2 = 2$ GeV^2 and $W^2 = 200$ GeV^2. The transverse photon cross section is dominating over the whole transverse momentum region.

This fragmentation function has been successful in describing experimental data of heavy flavored hadrons and can be easily understood in the following way. The transition amplitude is proportional to the inverse energy difference ΔE between the initial heavy quark Q and the final meson h plus light quark state q

$$\begin{aligned} \Delta E &= E_Q - E_h - E_q \\ &= \sqrt{m_Q^2 + P^2} - \sqrt{m_h^2 + z^2 P^2} - \sqrt{m_q^2 - (1-z)^2 P^2} \\ &\approx \frac{m_Q^2}{2P}\left(1 - \frac{1}{z^*} - \frac{e_Q}{1-z^*}\right) , \end{aligned} \tag{48}$$

where $m_h = m_Q$ can be used for simplicity. The fragmentation function is given by the square of the transition amplitude normalized correctly. The Peterson parameter $e_Q = m_q^2/m_Q^2$ parametrizes the hardness of the fragmentation and is fitted to data. The larger the quark mass, the smaller is ϵ_Q and the harder is the fragmentation, i.e. $D_Q^h(z^*)$ is peaked more towards $z^* = 1$. The z-integrals of the Peterson fragmentation functions D_Q^h are normalized to the branching ratios f_Q^h which summed over all hadron species add up to unity

$$\sum_h f_Q^h = \sum_h \int D_Q^h(z^*) dz^* = 1. \tag{49}$$

In general we are using the branching ratios given in Ref. [13] which refer to the specific

kinematical domain of the H1-experiment. The world averages evaluated by the Particle Data Group [14] are also listed in Table (II) for comparison. The large isospin violating branching ratio for the D^0-meson compared with the D^+-meson branching ratio comes from the accidental nearness of the D*-resonances to the sum of the masses of the D-meson and a pion. Namely both the D^{*+} and D^{*0} can decay into D^0 with large branching fractions, but the D^{*+} can only decay to the D^+ with a small branching. The Peterson parameter for the charm fragmentation function is $\epsilon_c = 0.05$ in the leading-logarithmic approximation (LLA) [15]. Although the branching ratios into D-mesons and D^*-mesons are approximately equal, it is much easier to measure D^*- mesons than D-mesons at HERA, since D^*-mesons have a good signature due to their $D^* \to D\pi \to K\pi\pi$ decay chain. The fits are performed with data from 'clean' e^+e^- reactions. We use these functions in DIS assuming independence from the underlying production process of the heavy quark.

$c \to$	D^0	D^+	D^{*0}	D^{*+}
PDG	0.565 ± 0.032	0.246 ± 0.020	0.213 ± 0.024	0.224 ± 0.028
H1	0.658 ± 0.054	0.202 ± 0.020	–	0.263 ± 0.019

TABLE II: Branching ratios $c \to D$ for several D-mesons. Reference values from Particle Data Group PDG [15] and H1 [13]. The H1 data is fitted without theoretical constraints due to the experimentally covered kinematical region.

The fragmentation process of bottom quarks requires a harder fragmentation function since the b-quark mass is 4-4.4 GeV, i.e. about 3.5 times larger than the charm quark mass. The reference value $\epsilon_b = 0.006$ for the bottom quark is therefore much smaller in the leading logarithmic approximation. The attachment of a light quark degrades the bottom quark momentum less than the charm quark momentum. The LLA-Peterson fragmentation functions are plotted for both flavors in Fig. 5.

When a high-momentum charm quark in the photon fragments into a charmed meson without additional transverse momentum, the scaling variable z^* gives the transverse and longitudinal fractions $p_c^\perp/p_D^\perp = p_c^L/p_D^L = 1/z^*$ at the same time. One finds:

$$< p_c^\perp/p_D^\perp >= \sum_h \int_0^1 \frac{dz^*}{z^*} D_c^h(z^*)$$

a mean ratio of transverse momenta $< p_c^\perp/p_D^\perp >= 1.68$ and $< p_b^\perp/p_B^\perp >= 1.29$ for the bottom sector, respectively. This makes the differential cross sections of the heavy quark harder than

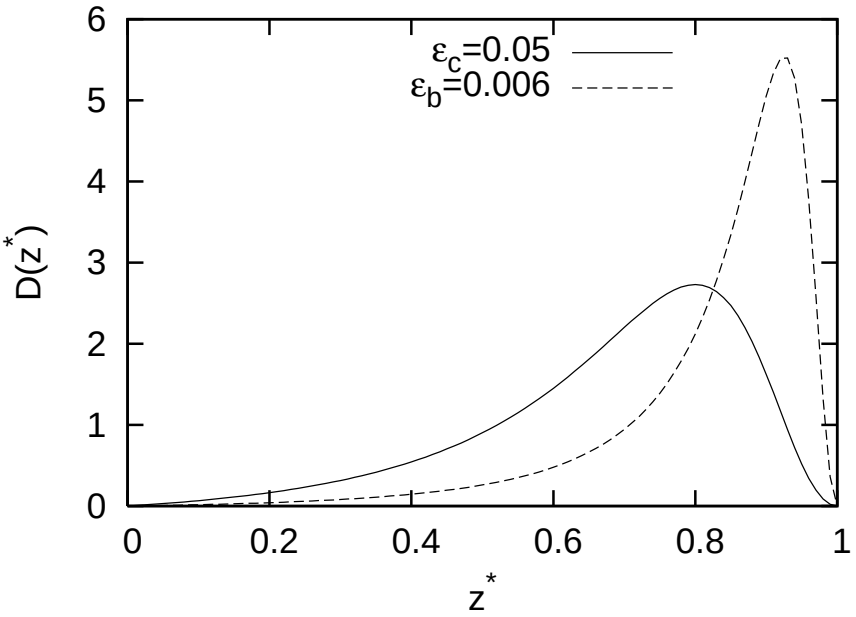

FIG. 5: The Peterson fragmentation function with $\epsilon_c = 0.05$ for charm quarks and $\epsilon_b = 0.006$ for bottom quarks in the leading log approximation. The bottom quark fragmentation is harder since the bottom quark mass is about 3.5 times higher than the charm quark mass. Both curves are normalized to unity.

the meson cross sections by the corresponding ratios. In order to see how the fragmentation acts we plot the longitudinal $\gamma^* p$ cross section $d\sigma^L/d^2p_t^2$ for the two different values of ϵ_Q as a function of the transverse momentum in Fig. 6. One sees how harder fragmentation functions shift the curve to higher transverse momenta.

V. COMPARISON WITH EXPERIMENTAL DATA

We evaluate numerically the ep cross section (23) for the H1 experiments [13, 16] at HERA taking into account the experimental cuts. In order to specify these cuts we use two different coordinate systems, the K-system and the K*-system: The z-axis of the K-system points in the incoming electron beam direction. The z-axis of the K*-system points in the photon direction. The experimental results of the measurements by the H1 collaboration are given in the K-system, i.e. with respect to the electron beam. The photon virtuality varies $2 < Q^2 < 100\,\mathrm{GeV}^2$, the inelasticity $0.05 < y < 0.7$ and pseudorapidity $|\eta(D)| \leq 1.5$.

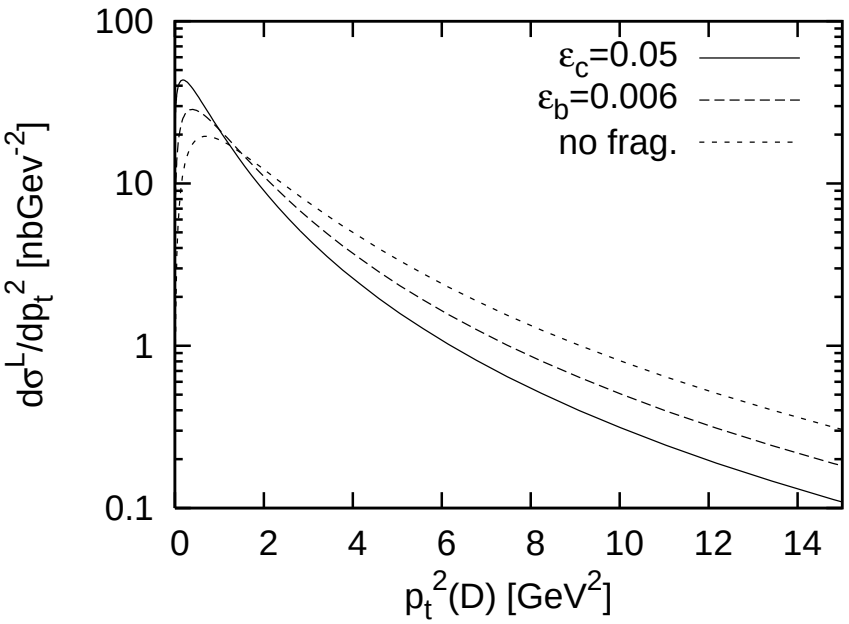

FIG. 6: The longitudinal heavy meson production cross section $\gamma^* p \to h(Q)X$ induced by longitudinal photons as a function of the transverse momentum of the meson. The two ϵ parameters correspond to charm ($\epsilon_c = 0.05$) and bottom quark ($\epsilon_b = 0.006$) fragmentation. For comparison we also show the transverse quark production cross section without fragmentation.

Further the minimum transverse momentum $p_{D\,min}^{\perp}$ is 2.5 GeV for the center-of-mass energy $\sqrt{s}$ =319 GeV [13] and $p_{D\,min}^{\perp} = 1.5$ GeV for $\sqrt{s} = 300$ GeV [16]. The theoretical dipole cross sections we use include well this Q^2-range. Our calculation, however, extrapolates somewhat the Bjorken-x range used in the GBW dipole cross section. The GBW range includes the x_B-interval $[10^{-4}, 10^{-2}]$, the experimental data spread over the larger interval $[10^{-5}, 0.02]$. Therefore the theoretical results for the smallest x_B values should be regarded with caution. We convert the differential cross section for electron-proton scattering (23) to the experimentally given variables. For x,y,Q^2 we use the relation $s = m_e^2 + M_P^2 + Q^2/(xy)$, i.e. $Q^2 = xys$ in the high-energy approximation. The rapidity is approximated by the pseudo-rapidity, $y_{rap.} \simeq \eta$. In the target rest frame (TRF) where $p_D^0 = m_T \cosh\eta$ and $\nu = ys/(2M)$, the z-fraction of the D-meson is calculated as follows

$$z = \frac{P \cdot p_D}{P \cdot q} \stackrel{\text{TRF}}{=} \frac{p_D^0}{\nu} = \frac{2M}{ys} m_T \cosh\eta \; . \tag{50}$$

We evaluate the differential D^+-cross sections with respect to the photon virtuality

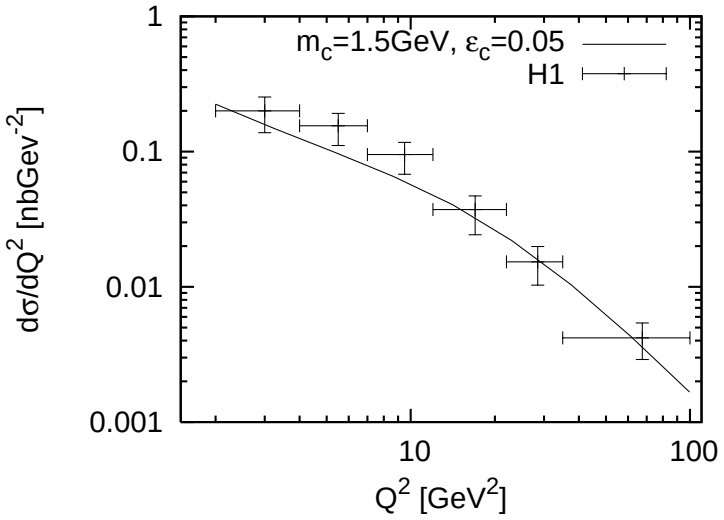

FIG. 7: Theoretical cross section $d\sigma(ep \to D^+X)/dQ^2$ with branching ratio $f_c^{D^+} = 0.202$ plotted against experimental data from reference [13]. Note, the experimental lower cut for the transverse momentum is $p_{D,min}^{\perp} = 2.5$ GeV.

$d\sigma/dQ^2$ and the rapidity of the D^+-meson $d\sigma/d\eta$. For both cross sections we integrate over the $p_D^{\perp}$ range inside the experimental cuts. In Fig. 7 we show $d\sigma(ep \to D^+X)/dQ^2$ for $\epsilon_c = 0.05$ and $m_c = 1.5$ GeV and compare with the H1 data [13]. The Q^2-decrease is determined by the integrals (c.f. eq. (42)) over the Bessel functions $K_{0,1}(\epsilon r)$ depending on the inverse extension parameter $\epsilon^2 = \alpha(1-\alpha)Q^2 + m^2$. With increasing photon virtuality Q^2, the Bessel functions damp the size of the cross section.

In Fig. 8 we plot the $d\sigma(ep \to D^+X)/d\eta$ cross section against the H1 data [13]. For the total cross section, higher quark masses would result in a lower η distribution. This holds for the whole rapidity range, even more so at mid rapidity. The whole curve becomes higher for a harder fragmentation. This is expected since the differential cross section falls off for high rapidities of either sign. Better data are announced [17] to come out for D*-mesons. In order to obtain theoretical predictions for other D-mesons one just has to multiply the D^+ cross section with the appropriate ratio of branching ratios (c.f. Table II). For example by multiplying the D^+ cross section with 2.6 one obtains the combined D^{*+}, D^{*-} cross sections.

Figure 9 shows the theoretical $d\sigma(ep \to D^*X)/dp_D^{\perp}$ cross section against the H1 data [16]. Our theoretical cross section reproduces the data adequately. It tends, however, to undershoot the cross section at large p_T. This would mean that the gluons in the proton have too

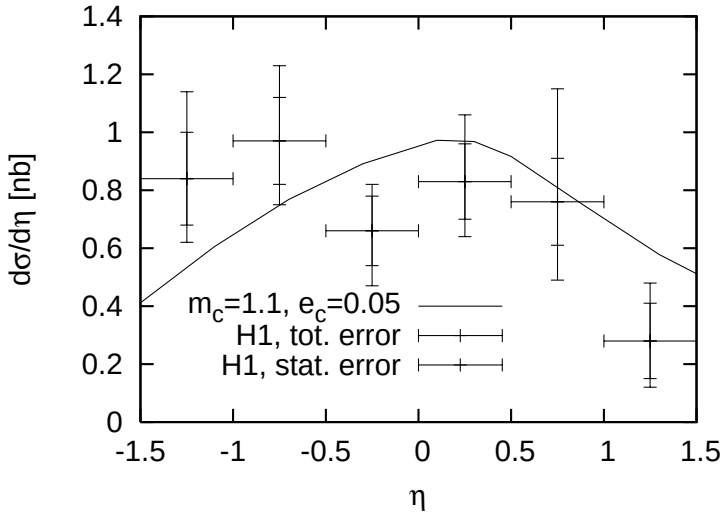

FIG. 8: Theoretical cross section $d\sigma(ep \to D^+X)/d\eta$ with branching ratio $f_c^{D^+} = 0.202$ plotted against experimental data from Ref. [13].

small transverse momenta or the unintegrated gluon density $f_G(x, \vec{k}_\perp)$ underestimates large transverse momenta. Indeed, the GBW parametrization for the dipole cross section leads to a Gaussian k_T-dependence for the unintegrated gluon density, while a power dependence is expected in QCD.

We have also investigated the dependence on the hardness of the fragmentation process. Our calculation is not very sensitive to changes of the Peterson parameter ϵ_c. A harder fragmentation lifts the differential cross section for transverse momenta above ~ 1.5 GeV and reduces it for lower ones.

VI. SUMMARY AND OUTLOOK

In this paper the color dipole model has been applied to the production of heavy flavored mesons in semi-inclusive deep inelastic scattering. In particular, transverse momentum distributions are a more valuable source of information about the production and fragmentation processes than total charm production. In the target rest frame, the virtual photon splits into a heavy quark-antiquark pair which subsequently scatters off the target. A color dipole is the lowest Fock state of the virtual photon. Instead of considering higher Fock states containing gluons, which become more important for lower x, these contributions are absorbed

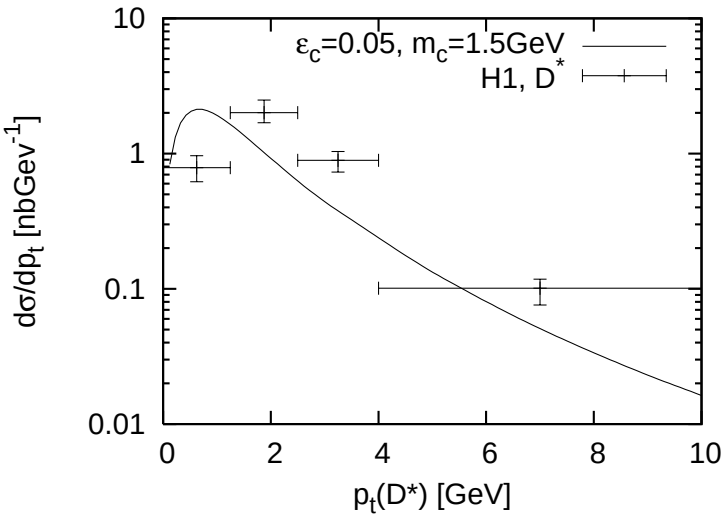

FIG. 9: Theoretical cross section $d\sigma(ep \to D^{*+}X)/dp_D^{\perp}$ with branching ratio $f_c^{D^{*+}} = 0.263$ plotted against experimental data from reference [16].

into the x-dependence of the dipole fit. The dipole formulation is in a mixed representation, where the longitudinal momentum is treated in momentum space and the transverse position in coordinate space. For high energies, the quark-antiquark pairs with fixed separation are interaction eigenstates. This formulation is very convenient for treating multiple scattering effects. With the help of the framework developed in this paper one can also calculate nuclear effects on heavy quark production by replacing the dipole-proton cross section by the dipole-nucleus cross section in Glauber approximation. For electroproduction on the proton we find a differential cross section in Q^2 which agrees well with H1 data. The large phase space coverage helps to collect sufficient statistics in the experiment. On the other side it presents a real challenge for the theoretical parametrization of the dipole cross section. In this respect the parametrization of Golec-Biernat and Wüsthoff's has a clear advantage compared with other approaches due to its wide kinematical applicability. It would be interesting to see the effects of the improved GBW dipole cross section [18] on the calculations. Inclusion of these corrections into the dipole description of direct photon production [19] reduces the cross section at high-p_T. Nevertheless, our results suggest that the dipole cross section is not the main source of deviations.

The fragmentation function has a stronger influence on the shape of the transverse momentum distribution. We get good fits with a rather hard fragmentation function. Since

there is no previous work which combines hadronization with the dipole approach, it is worthwhile to investigate how to treat heavy quark production and fragmentation consistently. Our fitted dipole cross section contains higher twist effects, i.e. it includes many soft gluons in the partonic cross section. Therefore we propose to use a fragmentation function at a low scale without evolution. We do not consider evolution which may become important at $p_D^\perp \gg m_c$.

Intrinsic transverse momenta of the target gluons are encoded into the dipole cross section. A primordial transverse momentum of the projectile gluon is often introduced in parton model, even in NLO calculations to harden the spectrum. Usually the primordial momentum substantially exceeds the typical hadronic scales. This is not necessary in the color dipole model, which generates the intrinsic gluon transverse momenta automatically (e.g. see in [20]).

Similar calculation can be applied to hadron induced production of charm [21]. While the total cross section of charm production in pp collisions is well explained [22], it remains to be seen how well p_T distribution can be explained in the same framework. Once it is possible to reduce the errors arising from hadronization, one may obtain more detailed information about the accuracy of the underlying dipole calculation.

Within the same dipole formalism one can calculate charm production in diffractive DIS, $l + p \to l' + \bar{c}c + p$. This cross section turns out to be a higher twist, $\sim 1/m_c^4$. However, semi-inclusive diffractive production, $l + p \to l' + \bar{c}cX + p$, is a leading twist, $\sim 1/m_c^2$ due to additional gluon radiation. It was demonstrated recently [23] that diffractive hadroproduction of heavy flavors is also a leading twist, and dipole model calculations well explain available data.

Acknowledgment

This work was partially supported by BMBF (Germany) grant 06HD158; by DFG (Germany) grant PI182/3-1; and by Fondecyt (Chile) grant 1050519.

APPENDIX A: EXPERIMENTAL CUTS

The experimental cuts are given with respect to the electron beam line. We relate the transverse momenta relative to the electron beam line and the virtual photon. As shown in

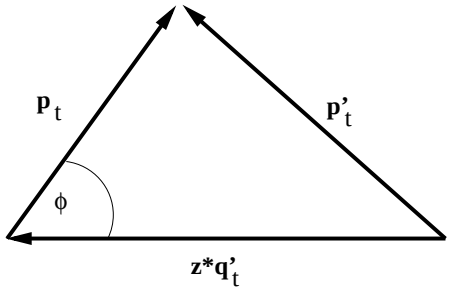

FIG. 10: Relating transverse momenta relative to the electron beam line, $p_D^{\perp\prime}$, and to the virtual photon direction $p_D^{\perp}$ for a small rotation of the z axis.

Fig. 10 we can write

$$\begin{aligned} \vec{p}_D^{\,\perp\prime} &= \vec{p}_D^{\,\perp} + \frac{z}{\alpha}\vec{q}_t' \\ &= \begin{pmatrix} p_D^x \\ p_D^y \end{pmatrix} + \begin{pmatrix} -\frac{z}{\alpha} q_t' \\ 0 \end{pmatrix} \end{aligned} \tag{A1}$$

and therefore

$$p_D^{\perp\prime} = \sqrt{\left(\frac{z}{\alpha}\, q_t'\right)^2 + (p_D^{\perp})^2 - 2\,\frac{z}{\alpha}\, q_t'\, p_D^{\perp}\,\cos\phi}\,, \tag{A2}$$

where the transverse virtual photon momentum q_t' is given by kinematics

$$q_t' = \frac{Q^2 M}{s}\sqrt{\frac{s^2}{Q^2\,M^2}(1-y) - 1} \tag{A3}$$

$$\simeq Q\sqrt{1-y}. \tag{A4}$$

The momenta are shown in Fig. 10. The quantities relative to the electron direction are indicated with a prime. The transverse photon momentum is accompanied by a factor $z/\alpha = z^*$. This factor evolves because the virtual photon splits into a heavy quark pair and not directly into D mesons.

[1] B.Z. Kopeliovich, L.I. Lapidus and A.B. Zamolodchikov, Sov. Phys. JETP Lett. **33**, 595 (1981); Pisma v Zh. Exper. Teor. Fiz. **33**, 612 (1981).

[2] J. Levelt and P.J. Mulders, Phys. Rev. D **49**, 96 (1994) [arXiv:hep-ph/9304232].

[3] J. Levelt, Deep inelastic semi-inclusive processes, PhD thesis, 1993.

[4] E. Berger, Proc. Workshop on electronuclear physics with internal targets, SLAC, eds. R.G. Arnold and R. Minehart, (1987).

[5] S.J. Brodsky, A. Hebecker and E. Quack, Phys. Rev. D **55**, 2584 (1997).

[6] J.D. Bjorken, J.B. Kogut and D.E. Soper, Phys. Rev. D **3**, 1382 (1971).

[7] B.Z. Kopeliovich, A. Schaefer and A. V. Tarasov, Phys. Rev. C **59**, 1609 (1999).

[8] B.Z. Kopeliovich, proc. of the workshop Hirschegg '95: Dynamical Properties of Hadrons in Nuclear Matter, Hirschegg January 16-21, 1995, ed. by H. Feldmeyer and W. Nörenberg, Darmstadt, 1995, p. 102 [arXiv:hep-ph/9609385].

[9] A.I. Shoshi, F.D. Steffen and H.J. Pirner, Nucl. Phys. A **709**, 131 (2002) [arXiv:hep-ph/0202012].

[10] K. Golec-Biernat, M. Wüsthoff, Phys. Rev. D **59**, 014017 (1999) [arXiv:hep-ph/9807513].

[11] R. Devenish, A. Cooper-Sarkar, "Deep Inelastic Scattering", Oxford University Press 2004.

[12] C. Peterson, D. Schlatter, I. Schmitt and P.M. Zerwas, Phys. Rev. D **27**, 105 (1983).

[13] H1 Collab., A. Aktas et al., Eur. Phys. J. C **38**, 447-459, 08/04 (2005).

[14] W.M. Yao *et al.* [Particle Data Group], J. Phys. G **33**, 1 (2006).

[15] S. Eidelmann et al., Phys. Lett. B **592**, 1 (2004).

[16] H1 Collaboration, C. Adloff et. al., Nucl. Phys. B **545**, 21-44 (1999) [arXiv:hep-ex/9812023].

[17] M. Krueger, private communication.

[18] J. Bartels, K. Golec-Biernat and H. Kowalski, Phys. Rev. D **66**, 010001 (2002) [arXiv:hep-ph/0203258].

[19] B.Z. Kopeliovich, A.H. Rezaeian, H.J. Pirner and I. Schmidt, arXiv:0704.0642 [hep-ph].

[20] A.I. Shoshi, F.D. Steffen, H.G. Dosch and H.J. Pirner, Phys. Rev. D **66**, 094019 (2002) [arXiv:hep-ph/0207287].

[21] B.Z. Kopeliovich and A.V. Tarasov, Nucl. Phys. A **710**, 180 (2002).

[22] B.Z. Kopeliovich and J. Raufeisen, Lectures given at International School on Heavy Quark Physics, Dubna, Russia, 27 May - 5 Jun 2002 [arXiv:hep-ph/0305094].

[23] B.Z. Kopeliovich, I. Schmidt and A.V. Tarasov [arXiv: hep-ph/0702106].